Journal of Photochemistry and Photobiology A: Chemistry 150 (2002) 167–175

Journal of Photochemistry and Photobiology A:Chemistry

www.elsevier.com/locate/jphotochem

Syntheses of mixed ligands complexes of Ru(II) with 4,4′-dicarboxy-2,2′-bipyridine and substituted pteridinedione and the use of these complexes in electrochemical photovoltaic cells

S. Anandan, S. Latha, P. Maruthamuthu*

Department of Energy (Chemistry-Interdisciplinary), University of Madras, Guindy Campus, Chennai 600 025, Tamil Nadu, India

Received 6 November 2001; received in revised form 17 January 2002; accepted 6 February 2002

Abstract

The synthesis, spectral and photoelectrochemical studies of mixed ligand complexes of [Ru(dcbpy)$_2$(LL)]Cl$_2$, where LL = 2,4-(1,3-*N*,*N*′-dimethyl)pteridinedione (DMP), 6,7-dimethyl-2,4-(1,3-*N*,*N*′-dimethyl)pteridinedione (MDMP), 6,7-diphenyl-2,4-(1,3-*N*,*N*′-dimethyl) pteridinedione (PhDMP), dibenzo[h,j]-(1,3-*N*,*N*′-dimethyl)isoalloxazine (BIAlo), 6,7-bis(pyrid-2-yl)-2,4-(1,3-*N*,*N*′-dimethyl) pteridinedione (PyDMP) were carried out. These complexes were attached to sol–gel processed TiO$_2$ electrodes and the photocells fabricated were illuminated with polychromatic radiation in the presence of I_2/I_3^- as redox electrolyte. The incident photon to current conversion efficiency determined was found to be ∼20–48%. © 2002 Elsevier Science B.V. All rights reserved.

Keywords: TiO$_2$; Pterdinedione; Isoalloxazine; Dye sensitization; Solar cells

1. Introduction

In recent years, considerable amount of research in the field of photochemistry has been directed towards photochemical and photoelectrochemical processes applicable to solar energy conversion processes [1–6]. It is well known that photoelectrochemical cells could be used for solar energy conversion into electricity as well as for production of chemical fuels. The basic principles and mechanisms involved in such systems have been reviewed [7–10] elaborately.

At present, the most promising method for light to electrical conversion is via photosensitized TiO$_2$ nanocrystalline electrode with Ruthenium(II) polypyridyl complexes [11–15]. For the past several years, polypyridyl ruthenium(II) complexes containing 4,4′-dicarboxy-2,2′-bipyridine as a photosensitizer attached to nanocrystalline TiO$_2$ have been widely studied in solar energy conversion processes [12,16–29]. For example, *cis*-bis(thiocyanato)bis(2,2′-bipyridyl-4,4′-dicarboxylato) Ru(II) is found to be an outstanding solar light absorber and charge transfer sensitizer [16,30–32] unmatched by any other dyestuff known so far. A good understanding of the charge transport in the nanostructured materials is of great importance for the development of an efficient solar cell. Different mechanisms for the charge transport have been discussed [33–38].

In nature, many biologically important compounds take part in electron transfer processes and act as one electron or two electron transfer agents. For instance, Flavin coenzymes transfer electrons to and from heme and iron–sulfur and molybdenum centers in proteins. They also serve as a required electron pair splitting or joining interface between metal one-electron donors or acceptors and organic two electron oxidants or reductants [39–41]. Pteridines are fused-ring nitrogen heterocyclic compounds that form the core structure of folates. They are found to function as cofactors for enzymes involved in hydroxylation [42] and methyl transfer [43,44]. They also act as redox mediator [45] and pigments for eyes and wings in certain insects [46] and in synthesis of anticancer drug [47,48]. The majority of the naturally occurring pteridine compounds have the 2-amino-4-oxo substitution pattern on the bicyclic core and have the trivial class name pterin. Fusion of a third benzene ring to a 2,4-dioxo-substituted pteridine group produces the core structure of the isoalloxazines, of which flavins are a subgroup. Certain enzymes for which pterins are cofactors,

---

* Corresponding author. Fax: +91-44-2352-494.
E-mail addresses: pmaruthu@satyam.net.in, pmaruthu@yahoo.com (P. Maruthamuthu).

PII: S1010-6030(02)00094-1

also require a metal for catalytic activity [49–51]. Various studies have been carried out to systematize the nature of transition metal co-ordination to folates and pteridines [52–54], flavins [55–60] and isoalloxazines [61,62]. Pterin and pteridine complexes containing biologically relevant metal ions Fe(II), Fe(III), Cu(II), Cu(I), Mo(VI) were prepared and studied [63,64]. Clarke et al. [65] have reported the structural, spectroscopic, and electrochemical studies of stable ruthenium(II) isoalloxazine complexes. Selective labeling of either the isoalloxazine or adenine rings of the flavin adenine dinucleotide (FAD) coenzyme or related coenzymes by coordination with Ru^{103} or Ru^{97} has yielded radio-pharmaceuticals which are of use as organ-imaging agents for diagnostic purposes [66–68].

The current work demonstrates the ability of Ru(II) to bind with pteridine and isoalloxazine ligands. We have attempted to synthesize and characterize stable new mixed ligand ruthenium polypyridyl complexes using 2,4-dioxopteridinediones as spectator ligands, of general formula $[Ru(dcbpy)_2(LL)]Cl_2$, where LL = 2,4-(1,3-*N*,*N*′-dimethyl)pteridinedione (DMP), 6,7-dimethyl-2,4-(1,3-*N*,*N*′-dimethyl)pteridinedione (MDMP), 6,7-diphenyl-2,4-(1,3-*N*,*N*′-dimethyl) pteridinedione (PhDMP), dibenzo[h,j]-(1,3-*N*,*N*′-dimethyl) isoalloxazine [BIAlo], 6,7-bis(pyrid-2-yl)-2,4-(1,3-*N*,*N*′-dimethyl)pteridinedione [PyDMP].

A number of ruthenium sensitizers with increased absorption coefficients for enhanced light harvesting are synthesized. For Ruthenium diimine sensitizers, the MLCT absorption can be extended to longer wavelengths by making suitable substituent changes on chromophoric ligands or by decreasing the $d\pi$–$d\pi^*$ backbonding donation to non-chromophoric ligands [69]. Argazzi et al. [70] have utilized dithiocarbamates as non-chromophoric chelating ligands in ruthenium complexes to tune sensitizer absorption property. The complexes that so far have shown the most promising characteristics are based on ruthenium polypyridyl moieties incorporating negative monodentate ligand. The presence of monodentate ancillary ligand can however lead to photochemical instability of the dye molecule. The complexes reported in this work are found to possess greater light absorption at longer wavelengths when anchored to nanocrystalline TiO_2 electrodes and their application for the purpose of conversion of light into electricity in regenerative solar cells has not been studied so far.

2. Experimental

2.1. Materials

All chemicals used in the preparation were of the purest research grade. $RuCl_3$, 2,3-butanedione (Fluka), 9,10-phenanthrenequinone, 1,3-dimethyl-5,6-diaminouracil, 2,2′-pyridil (Aldrich) were used as such. The solvents were purified and dried according to standard methods [71]. 4,4′-Dicarboxy-2,2′-bipyridine (dcbpy) was prepared from 4,4′-dimethyl-2,2′-bipyridine (Aldrich) according to the method described by Garelli and Vierling [72]. TiO_2 (Degussa; surface area 55 m^2/g measured by Carlo Erba Strumentazione instrument) and Triton X-100 (Aldrich) were used.

2.2. Preparations of ligands

The substituted pteridinedione ligands from Uracil are prepared as in Scheme 1. The ligands (**1–5**) are prepared by condensing 1,3-dimethyl-5,6-diaminouracil (1.7 g) with reactants glyoxal (0.58 g), 2,3-butanedione (0.86 g), benzil (2.1 g), 9,10-phenanthrenequinone (2.08 g) and 2,2′-pyridil respectively, in ethanol (25 ml) and the mixture refluxed for 5 h. The precipitate formed was filtered and washed with alcohol several times and finally dried with diethyl ether.

The structure of the ligands (**1–5**) was confirmed by spectroscopic data such as UV–visible, IR, ^1H, ^{13}C NMR, mass spectra and elemental analysis.

2.2.1. DMP

Data: UV–visible (CH_3OH) λ_{max} (nm) 364; IR (KBr pellet) C=O group 1710, 1693 cm^{-1}; ^1H NMR ($CDCl_3$/TMS; ppm): δ 8.63 (s, 2H) and N–CH_3 (s, δ 3.72 and 3.52); ^{13}C NMR (ppm): six peaks (δ 45.44, 50.23, 145.62, 148.42, 196.85, 197.55); *m*/*e*: 193; CHN analysis (calculated values in parentheses): %C 50.1 (49.79), %H 4.21 (4.16), %N 29.21 (29.17).

2.2.2. MDMP

Data: UV–visible (CH_3OH) λ_{max} (nm) 364, 270; IR (KBr pellet) C=O group 1715, 1676 cm^{-1}; ^1H NMR ($CDCl_3$/TMS; ppm): C–CH_3 (s, δ 1.23 and 1.635) and N–CH_3 (s, δ 3.72 and 3.52); ^{13}C NMR (ppm): eight peaks (δ 29.13, 29.93, 43.31, 49.32, 135.42, 145.32, 196.34, 197.25); *m*/*e*: 221; CHN analysis (calculated values in parentheses): %C 54.62 (54.55), %H 5.49 (5.45), %N 25.51 (25.45).

2.2.3. PhDMP

Data: UV–visible (CH_3OH) λ_{max} (nm) 444, 360; IR (KBr pellet) C=O group 1712, 1678 cm^{-1}; ar C–H (bending) 754 cm^{-1}; ^1H NMR ($CDCl_3$/TMS; ppm): N–CH_3 (s, δ 3.8 and 3.66), aromatic protons δ 7.31–7.9 (m, 10H); ^{13}C NMR (ppm): 13 peaks (δ 45.61, 49.23, 110.25, 115.24, 125.25, 129.56, 131.73, 135.59, 145.87, 153.37, 155.22, 196.15, 197.33); *m*/*e*: 345; CHN analysis (calculated values in parentheses): %C 69.7 (70.18), %H 4.6 (4.65), %N 16.47 (16.37).

2.2.4. BIAlo

Data: UV–visible (DMSO) λ_{max} (nm) 412, 266; IR (KBr pellet) C=O group 1720, 1670 cm^{-1}; ar C–H 773, 734 cm^{-1}; ^1H NMR (DMSO/TMS; ppm): N–CH_3 (s, δ 3.72 and 3.43), aromatic protons δ 6.31–7.82 (m, 8H); ^{13}C NMR (ppm): 13 peaks (δ 43.32, 48.54, 123.25, 125.24, 131.15, 133.56, 146.73, 153.59, 155.87, 158.37, 164.22, 196.2, 197.43); *m*/*e*:

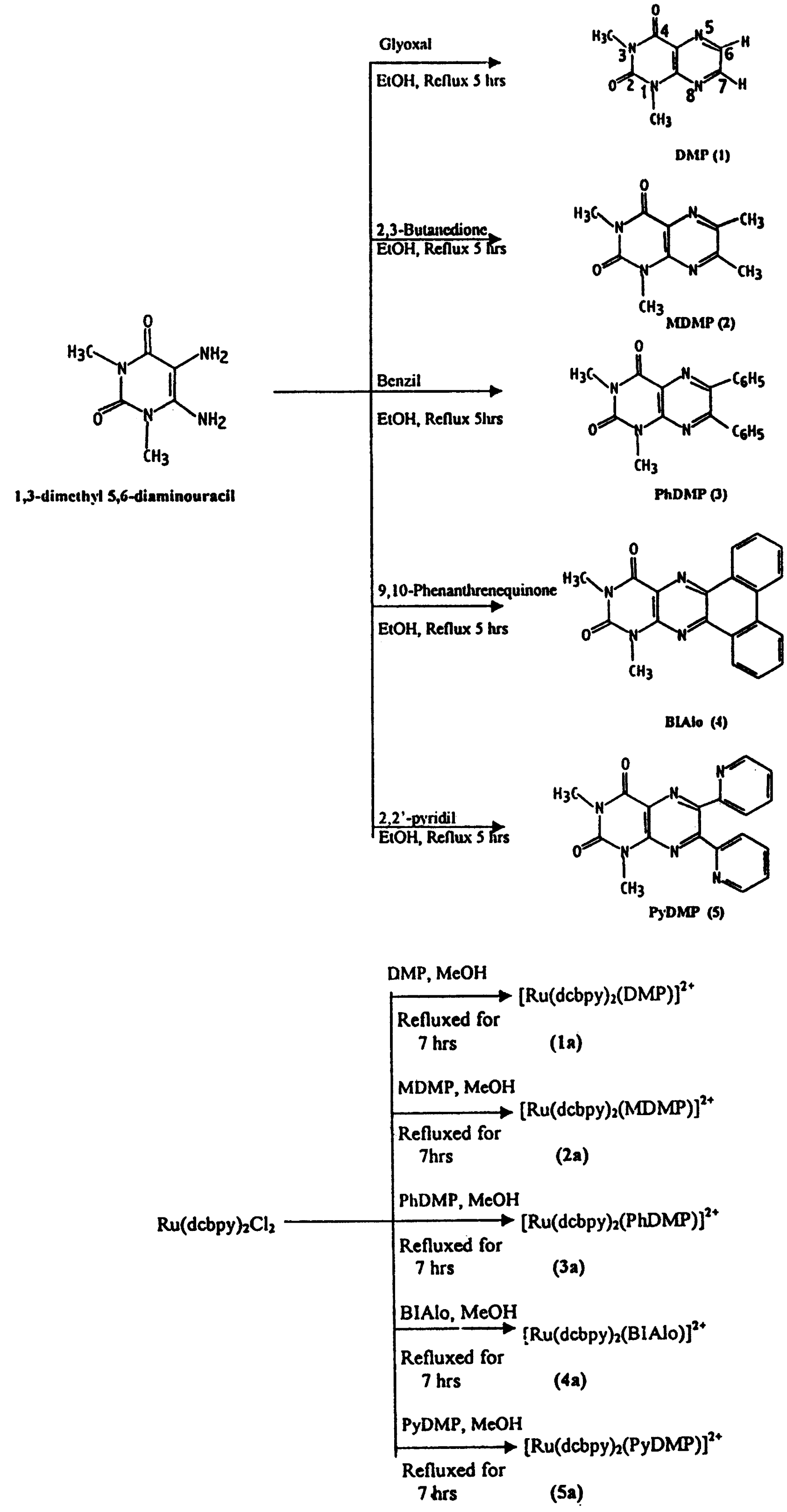
1,3-dimethyl 5,6-diaminouracil
Glyoxal
EtOH, Reflux 5 hrs
DMP (1)
2,3-Butanedione
EtOH, Reflux 5 hrs
MDMP (2)
Benzil
EtOH, Reflux 5hrs
PhDMP (3)
9,10-Phenanthrenequinone
EtOH, Reflux 5 hrs
BIAlo (4)
2,2'-pyridil
EtOH, Reflux 5 hrs
PyDMP (5)
Ru(dcbpy)2Cl2
DMP, MeOH
Refluxed for 7 hrs
[Ru(dcbpy)2(DMP)]2+
(1a)
MDMP, MeOH
Refluxed for 7hrs
[Ru(dcbpy)2(MDMP)]2+
(2a)
PhDMP, MeOH
Refluxed for 7 hrs
[Ru(dcbpy)2(PhDMP)]2+
(3a)
BIAlo, MeOH
Refluxed for 7 hrs
[Ru(dcbpy)2(BIAlo)]2+
(4a)
PyDMP, MeOH
Refluxed for 7 hrs
[Ru(dcbpy)2(PyDMP)]2+
(5a)

Scheme 1.

343; CHN analysis (calculated values in parenthesis): %C 69.8 (70.18), %H 4.13 (4.09), %N 16.42 (16.37).

2.2.5. *PyDMP*

Data: UV–visible (CH_3OH) λ_{max} (nm) 358, 272; IR (KBr pellet) C=O group 1720, 1676 cm^{-1}; ^1H NMR ($CDCl_3$/TMS; ppm): δ 8.78 (m, 2H), 8.36 (m, 2H), 8.02 (m, 2H), 7.8 (m, 2H) and N–CH_3 (S, δ 2.53 and 3.02); ^{13}C NMR (ppm): 11 peaks (δ 40.78, 50.57, 111.24, 126.25, 128.56, 128.73, 133.59, 162.87, 166.37, 196.85, 197.55); *m*/*e*: 347; CHN analysis (calculated values in parentheses): %C 62.35 (62.43), %H 4.03 (4.05), %N 24.2 (24.28).

2.3. *Synthesis of [Ru(dcbpy)$_2$(LL)]Cl$_2$ complexes*

The 0.152 mmol of ligands (**1**–**5**) was added to 0.152 mmol of the complex *cis*-Ru(dcbpy)$_2$Cl$_2$ in 25 ml of methanol. The resulting mixture was refluxed for 7 h in Argon atmosphere. The solution was cooled, filtered and the solvent was removed from the filtrate using rotary evaporator. The solid thus isolated was washed with dry acetone and dried. The solid was recrystallized from ethanol–water mixture and dried. Elemental analysis of complexes were determined using Heraeus CHN Rapid Analyzer.

2.3.1. *[Ru(dcbpy)$_2$(DMP)]Cl$_2$·3H$_2$O (**1a**)*

Data: IR (KBr pellet) C=O group 1674, 1712 (w) cm^{-1}; CHN analysis (calculated values in parentheses): %C 41.97 (42.3), %H 3.23 (3.31), %N 11.91 (12.36).

2.3.2. *[Ru(dcbpy)$_2$(MDMP)]Cl$_2$·3H$_2$O (**2a**)*

Data: IR (KBr pellet) C=O group 1672 (w), 1718 (w) cm^{-1}; CHN analysis (calculated values in parentheses): %C 43.85 (43.68), %H 3.71 (3.64), %N 12.25 (11.99).

2.3.3. *[Ru(dcbpy)$_2$(PhDMP)]Cl$_2$·3H$_2$O (**3a**)*

Data: IR (KBr pellet) C=O group 1678 cm^{-1}; CHN analysis (calculated values in parentheses): %C 49.7 (49.9), %H 3.47 (3.59), %N 10.65 (10.59).

2.3.4. *[Ru(dcbpy)$_2$(BIAlo)]Cl$_2$·3H$_2$O (**4a**)*

Data: IR (KBr pellet) C=O group 1631, 1714 (m) cm^{-1}; CHN analysis (calculated values in parentheses): %C 49.81 (50.0), %H 3.48 (3.41), %N 10.72 (10.6).

2.3.5. *[Ru(dcbpy)$_2$(PyDMP)]Cl$_2$·3H$_2$O (**5a**)*

Data: IR (KBr pellet) C=O group 1674, 1720 cm^{-1}; CHN analysis (calculated values in parentheses): %C 47.21 (47.65), %H 3.33 (3.4), %N 13.12 (13.21).

2.4. *Physical measurements*

The UV–visible and infrared absorption spectra were recorded (Shimadzu 1601 spectrophotometer and Shimadzu FT-IR 8000 spectrophotometer). ^1H and ^{13}C NMR were recorded on Brauker 400 mHz instrument using TMS as internal standard. The electron impact (EI) ionization mass spectrometry (Jeol-JMS-DX 303HF) instrument was used to determine the mass of the ligands. Cyclic voltammetric measurements were carried out with BAS 100 A electrochemical system. The three-electrode assembly comprising of glassy carbon working electrode, platinum as auxiliary electrode and an SCE reference electrode were used. All electrochemical measurements were carried out with 3×10^{-4} M complex in dry ethanol. The reference electrode was in contact with 0.1 M LiCl in methanol and it was separated from the working electrode compartment by a bridge containing 0.1 M *n*-tetrabutylammoniumperchlorate in ethanol.

2.5. *Preparation of nanocrystalline TiO$_2$ films; dye coating of the electrode and surface roughness factor of the film*

Nanocrystalline TiO_2 film was prepared on the conducting glass support such as F:SnO_2, ITO and ZnO as reported [12]. Coating the TiO_2 surface with the dye was carried out by dipping the electrode (maintained at ∼80 °C) in a 3×10^{-4} M solution of the ruthenium complex in ethanol for 24 h. During this time, the surface changed from white to the color of the attached dye. After the completion of the dye adsorption, the electrode was withdrawn from the solution under a stream of argon.

The roughness factor of the TiO_2 electrode [13] was determined from the amount of the dye adsorbed on it. The amount of the adsorbed dye was determined by desorbing the dye from the TiO_2 surface into a solution of 10^{-2} M NaOH and measuring its absorption. The original surface coverage of the electrode was subsequently calculated from the geometric electrode area and the amount of detached complex in solution determined through spectrophotometric analysis.

The regenerative photoelectrochemical cell consisted of the dye loaded TiO_2 film deposited on transparent conducting glass support and a conducting glass sheet (SnO_2 (sheet resistance 10 Ω/cm^2), ITO and ZnO (sheet resistance 20 Ω/cm^2)) loaded with a thin platinum film serving as the counter electrode and iodine/iodide redox electrolyte. The electrodes were clipped together and illuminated through the TiO_2-sensitized surface with tungsten halogen lamps of varying intensities (1.2 and 2.5 mW/cm^2). The short circuit photocurrent (I_{SC}), open circuit photovoltage (V_{OC}) and fill factor were measured from the above two electrodes arrangement. The intensity of incident light was measured by chemical actinometry using ferric oxalate [73].

3. Results and discussion

3.1. *Absorption spectra*

The absorption spectra for the complexes **1a**–**5a** in ethanol are summarized in Table 1. The interesting feature of these

Table 1
Absorption, electrochemical and adsorption data of $[Ru(dcbpy)_2(LL)]^{2+}$ complexes

Complex	λ_{max} (nm), ε ($\times 10^3\ M^{-1}\ cm^{-1}$)	E_{pa} (mV)	Surface concentration Γ (mol/cm^2)
$[Ru(dcbpy)_2(DMP)]Cl_2$	514 (2.2), 362 (sh), 314 (16.8)	700	0.85×10^{-7}
$[Ru(dcbpy)_2(MDMP)]Cl_2$	550 (7.5), 400(sh), 364 (17), 316 (25.7), 246 (30)	820	1.2×10^{-7}
$[Ru(dcbpy)_2(PhDMP)]Cl_2$	552 (3.3), 410 (sh), 366 (8.4), 314 (26.7)	717	1.5×10^{-7}
$[Ru(dcbpy)_2(BIAlo)]Cl_2$	532 (5.2), 388 (6.15), 314 (15.5)	900	1.8×10^{-7}
$[Ru(dcbpy)_2(PyDMP)]Cl_2$	512 (0.56), 440 (0.75), 355 (0.22), 300 (0.34)	780	1.18×10^{-7}

complexes is a broad MLCT absorption band in the visible region with a maximum at 512–552 nm with the molar absorption ranging from 1170 to 7500 $M^{-1}\ cm^{-1}$. Fig. 1A–E shows the absorption spectra of ligands and their ruthenium complexes. The MLCT bands of these complexes are broad and red shifted compared to those of $[Ru(dcbpy)_3]^{4-}$ [74]. Thus the observed red shift could result from greater π-acceptor ability of the ligand or greater ease of back donation to the ligand [75–78]. The positions of the low energy maxima are also sensitive to the nature of the ligand, shifting to longer wavelength as the degree of π-delocalization in the acceptor ligand increases [79]. These complexes also exhibit strong UV band at around 360, 314 and 246 nm. The band at 360 nm is assigned to intraligand π–π^* transitions. Those at 314 and 246 nm are due to π–π^* transition of dcbpy ligands. The emission spectrum of complex **5a** is found to have a single band with a maximum at 602 nm. The lifetime of the excited state of the complex **5a** was found to be 11 ns at room temperature. The other complexes have very short-lived excited states (<5 ns).

3.2. Vibrational measurements

The structural determination of the complexes showed chelation of the pteridine unit through the exocyclic O-atom (O_4) and a pyrazine ring N-atom (N_5) [64,80] as observed in the metal complexes of flavins and isoalloxazines [65]. Similar observations were made in this work too. Infrared data for the ligands (**1**–**5**) reveal that in each case the intense absorption of the carbonyl group is present in the region 1650–1720 cm^{-1}. When the ligands (**1**–**4**) form Ru(II) (**1a**–**4a**) complexes, of the two distinct absorption of the carbonyl region, one mode disappears and the second mode occurs with less intensity at lower energies [57,61,62,64,80].

The IR spectrum for the complex (**5a**) shows intense absorption peaks of the carbonyl groups in the region (1674, 1720 cm^{-1}) and also that of ν(Ru–N–py) in the region of 262 cm^{-1} [81,82]. This may indicate that the coordination of Ru to the ligand PyDMP occurs through N_8 and N–py and do not involve oxygen atom.

3.3. Langmuir adsorption isotherm at the surface of TiO_2

For adsorption measurements, a solution of a complex in ethanol containing 0.25 g/l of TiO_2 powder was employed. From the Langmuir adsorption isotherm [83], the binding constants (K_b) for the complexes were found to be in the range $6.9–7.7 \times 10^4\ dm^3$/mole and the surface area requirement was 62–71 Å^2/molecule. The carboxylate groups adsorb specifically at the surface of TiO_2 resulting in the intimate contact required for efficient sensitization [84,85]. The interaction of the carboxylate group with the surface Ti ions is likely to lead to formation of –C–O–Ti– bonds. The carboxylate group serves as an interlocking group enhancing electronic coupling between the π^* orbital of 2,2′-bipyridine ring and Ti (3d) orbital of the semiconductor [86]. This coupling leads to increased delocalization of the π^* level of 2,2′-bipyridine ligand. The low binding constants of these complexes can be attributed to decrease in the extent of delocalization of π^* orbital of the bipyridine ligand upon adsorption of the complex at the surface of TiO_2 compared to $[Ru(dcbpy)_3]^{4-}$ [28].

A surface concentration of about 0.85×10^{-7} to $1.80 \times 10^{-7}\ mol/cm^2$ for the above complexes was spectrophotometrically measured. The low surface concentration of the complex **1a** could be due to the low solubility of the complex in ethanol [28]. According to the results of Furlong et al. [87], one $[Ru(dcbpy)_3]^{4-}$ molecule was found to occupy 100 Å^2 of TiO_2 surface at saturation monolayer coverage. On the basis of this area, the surface roughness factor was estimated as ∼700.

3.4. Electrochemical and photoelectrochemical measurements

The cyclic voltammogram of the complexes **1a**–**5a** show irreversible oxidation potentials in the region of 0.72–0.9 V (versus SCE, scan rate: 45 mV/s) for 3×10^{-4} M ethanolic solution. In polypyridyl complexes of Ru(II), the separation between the lowest polypyridine ligand (π^*) and Ru(t_{2g}) orbitals is the energy of MLCT. The MLCT state energy can thus be reduced either by decreasing the energy of ligand π^*-orbital or raising the energy of metal (t_{2g}) orbital. In general, the lower oxidation potential of the complexes $[Ru(dcbpy)_2(LL)]^{2+}$ compared to $[Ru(dcbpy)_3]^{4-}$ is due to increased electron donating properties of the ligand LL which pushes the dd-states to higher energy. This is in accordance with decrease in the energy of MLCT transition as observed in absorption spectra [88,89]. Also, the presence of lower π^* level of these ligands has lowered the oxidation potential of the complexes compared to 1.51 V of $[Ru(bpy)_2(pyr)_2]^{2+}$ [90]. The peak oxidation potential (E_{pa})

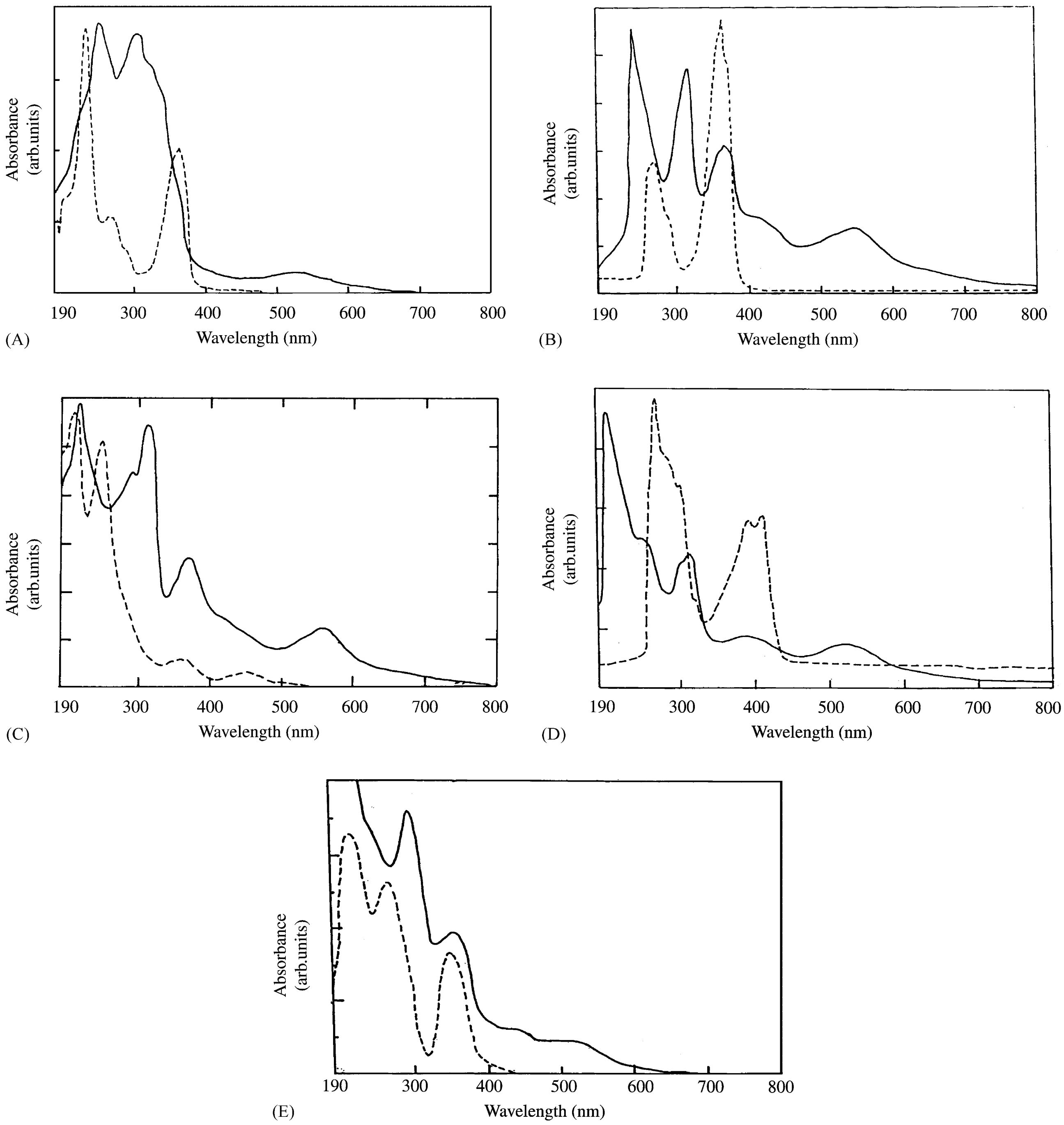

Fig. 1. (A) Absorption spectra of DMP ligand (- - -) and $[Ru(dcbpy)_2(DMP)]^{2+}$ (—). (B) Absorption spectra of MDMP ligand (- - -) and $[Ru(dcbpy)_2(MDMP)]^{2+}$ (—). (C) Absorption spectra of PhDMP ligand (- - -) and $[Ru(dcbpy)_2(PhDMP)]^{2+}$ (—). (D) Absorption spectra of BIAlo ligand (- - -) and $[Ru(dcbpy)_2(BIAlo)]^{2+}$ (—). (E) Absorption spectra of PyDMP ligand (- - -) and $[Ru(dcbpy)_2(PyDMP)]^{2+}$ (—).

of the complex **5a** is less positive than **2a** and **4a** which may be attributed to increased σ donor effect of pyridine ring of the ligand PyDMP, which enhances the energy of metal d-orbitals [91]. The anodic shift of the peak potential (E_{pa}) as in **4a** with increasing degree of π-delocalization on the ligand can be correlated with spectroscopic trends.

The results obtained on the photo-performance of ruthenium complexes as sensitizers on nanocrystalline TiO_2 electrodes have been presented in Table 2. The IPCE values of these dyes were calculated using the relation

$$\text{IPCE (\%)} = \frac{\text{photocurrent density } (I_{SC})\ (\text{mA/cm}^2) \times 1240}{\text{wavelength (nm)} \times \text{photon flux } (I_{inc})\ (\text{mW/cm}^2)} \times 100$$

Although TiO_2 shows only a weak response in the visible

Table 2
Photoelectrochemical properties of $[Ru(dcbpy)_2(LL)]^{2+}$ complexes

Complex	Glass	V_{OC} (mV)	I_{SC} (μA)	ff	IPCE(%)	η (%)
$[Ru(dcbpy)_2(DMP)]Cl_2$	SnO_2	289	315	0.55	33.24	2.0
	ITO	210	230	0.51	23.21	1.0
	ZnO	175	151	0.53	15.90	0.58
$[Ru(dcbpy)_2(MDMP)]Cl_2$	SnO_2	330	400	0.61	42.21	3.2
	ITO	215	285	0.63	30.07	1.5
	ZnO	173	190	0.59	20.05	0.77
$[Ru(dcbpy)_2(PhDMP)]Cl_2$	SnO_2	420	604	0.38	63.74	3.8
	ITO	340	450	0.40	47.48	2.9
	ZnO	260	325	0.35	34.29	1.2
$[Ru(dcbpy)_2(BIAlo)]Cl_2$	SnO_2	320	390	0.45	41.15	2.2
	ITO	232	270	0.38	28.49	0.94
	ZnO	187	200	0.41	21.11	0.61
$[Ru(dcbpy)_2(PyDMP)]Cl_2$	SnO_2	212	220	0.65	48.36	2.5
	ITO	157	175	0.61	38.40	1.4
	ZnO	110	111	0.63	24.10	0.63

region, $[Ru(dcbpy)_2LL]^{2+}$ coated TiO_2 electrodes exhibit high photocurrents. Polychromatic light was used to excite the TiO_2 film. Irradiation was performed from the front side through the conduction glass support. Efficiencies quoted refer to incident light intensities and are uncorrected for the light reflection, scattering and absorption by the glass sheet. The photocurrent densities for the complexes **1a**–**5a** ranging from 220 to 604 μA/cm^2 were measured at incident light intensities of 1.2–2.5 mW/cm^2 which correspond to IPCE values ranging from 33 to 48% on SnO_2 conducting glass. The IPCE values for all the sensitizers on TiO_2/ITO glass or TiO_2/ZnO glass are found to be quite low due to high internal resistance of the conducting glasses [92,93]. These sensitizers are not as efficient as $[Ru(dcbpy)_2(NCS)_2]$ [12].

Fig. 2 shows the current–voltage characteristics of a cell consisting of $[Ru(dcbpy)_2(BIAlo)]Cl_2$ coated 2 × 2 cm sized TiO_2 film as photoanode and platinum counter electrode. As the load resistance or voltage is increased, the current at first stays constant and then falls to zero at an open circuit voltage of 0.32 V. The maximum power (mW) delivered is represented by the area of the largest rectangle that can be fitted under the curve. Dividing this by the product of V_{OC} and I_{SC} gives the fill factor of the cell for which a value of 0.45 is obtained. Similarly, the fill factor for the other complexes were determined and tabulated (Table 2).

The observed fill factor and the open circuit voltage for the above complexes are rather low. The low values of V_{OC} can be explained due to dark current arising from the reduction of triiodide by conduction band electrons.

$$I_3^- + 2e_{cb}^-(TiO_2) \rightarrow 3I^-$$

This electrochemical reduction of triiodide ($E^\circ = 0.54$ V) plays an important role in influencing the performance characteristics of the cell [12]. There are various reasons for the high performance of $[Ru(dcbpyH_2)_2(NCS)_2]$ as sensitizer for solar cells. The π^* level allows quantitative charge injection into TiO_2 and although the absorption spectrum is shifted to longer wavelengths by –NCS ligands, the $Ru(t_{2g})$ level is not shifted too much for iodide regeneration [32]. Thus the fine-tuning of $Ru(t_{2g})$ level and π^* level appears very difficult. The understanding of the key parameters affecting cell performances is of relevance to the design of the molecular sensitizer. Although strong absorption in the visible part of the spectrum favors solar energy conversion processes, the excited state properties and the redox potential of the molecular dyes have to be tuned with respect to the level of the conduction band in the TiO_2 and to the redox potential of the sacrificial donor I^- in order to increase the driving force of the corresponding electron transfer processes. A general mechanism of sensitization in a regenerative solar cell is shown in Scheme 2.

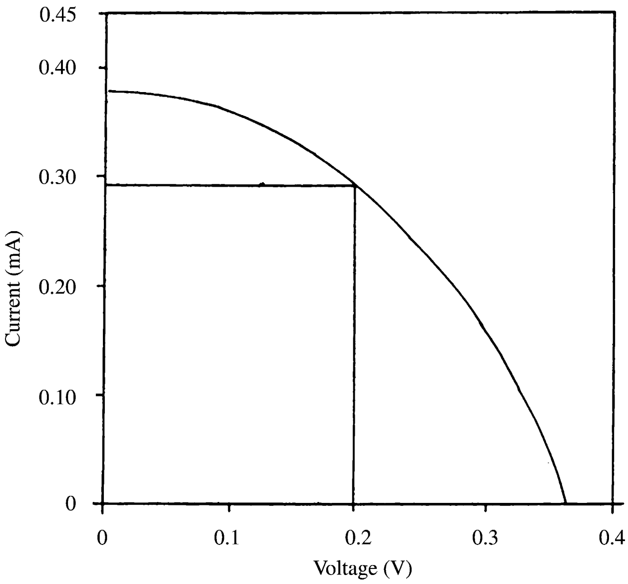

Fig. 2. Photocurrent–voltage characteristics for $[Ru(dcbpy)_2(BIAlo)]^{2+}$ on TiO_2 coated SnO_2 conducting glass.

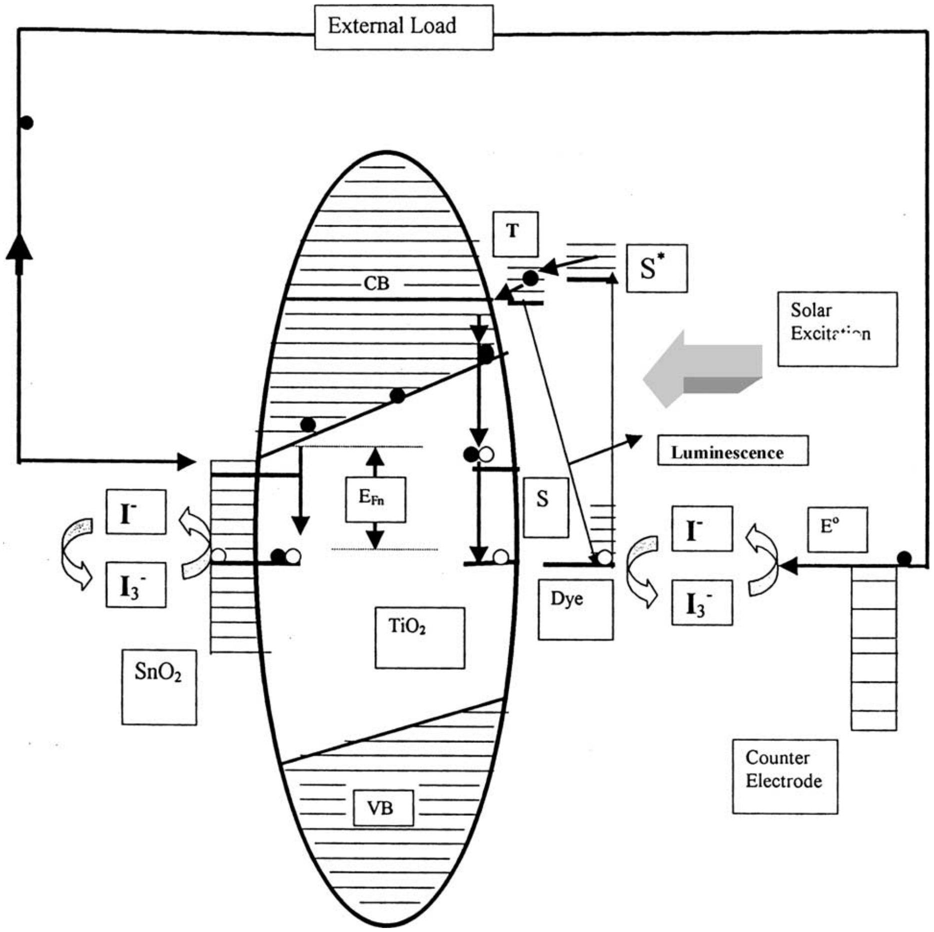

Scheme 2. Energy transfer phenomena of solar cell.

4. Conclusion

Ruthenium polypyridyl photosensitizers with substituted pteridine ligands have been synthesized and characterized. Anchored to nanocrystalline TiO_2 films, the sensitizers convert light into electricity in regenerative solar cells fabricated, over the entire visible region of the solar spectrum. $[Ru(dcbpy)_2(PhDMP)]^{2+}$ was found to be a better redox sensitizer because of its ability to harvest large fraction of visible light. It possesses very short excited state lifetime (<5 ns). All these complexes are found to be adsorbed on the surface of TiO_2 to a lesser extent than $[Ru(dcbpy)_2(NCS)_2]$. Consequently the ultra fast electron injection from the excited complex into the semiconductor may take place less effectively. However, from the current generated it may be inferred that the photoinjected electrons percolate rapidly through the film and are effectively collected by conducting glass support.

References

[1] K. Honda, A. Fujishima, Nature 238 (1972) 37.
[2] B.J. Tufts, Nature 326 (1987) 681.
[3] H. Gerischer, Electrochim. Acta 35 (1990) 1677.
[4] S. Licht, G. Hodus, R. Tenne, J. Mannassen, Nature 326 (1987) 863.
[5] H. Tributsch, J.C. Bennet, J. Electroanal. Chem. 81 (1977) 97.
[6] A.J. Bard, Science 207 (1980) 139.
[7] A.J. Nozik, Ann. Rev. Phys. Chem. 29 (1978) 189.
[8] L.A. Harris, R.H. Wilson, Ann. Rev. Mater. Sci. 8 (1978) 99.
[9] H. Gerischer, in: B.O. Seraphin (Ed.), Topics in Applied Physics, Vol. 31, Springer, Berlin, 1979, pp. 115–172.
[10] R. Memming, Electrochim. Acta 25 (1980) 77.
[11] B.O. Regan, M. Gratzel, Nature 353 (1991) 737.
[12] M.K. Nazeeruddin, M. Kay, I. Rodicio, R. Humphry-Baker, E. Muller, P. Liska, N. Vlachopoulos, M. Gratzel, J. Am. Chem. Soc. 115 (1993) 6382.
[13] T.A. Heimer, C.A. Bignozzi, G.J. Meyer, J. Phys. Chem. 97 (1993) 11987.
[14] G. Smestad, C.A. Bignozzi, R. Argazzi, Sol. Energy Mater. Sol. Cells 32 (1994) 259.
[15] R. Knoedler, J. Sopka, F. Harbach, H.W. Guenling, Sol. Energy Mater. Sol. Cells 30 (1993) 277.
[16] A. Hagfeldt, B. Didriksson, T. Palmquist, H. Lindstrom, S. Sodergren, H. Rensmo, S.E. Lindquist, Sol. Energy Mater. Sol. Cells 31 (1994) 48.
[17] P. Maruthamuthu, S. Anandan, Sol. Energy Mater. Sol. Cells 59 (1999) 199.
[18] B.O. Regan, J. Moser, M. Anderson, M. Gratzel, J. Phys. Chem. 94 (1990) 8720.
[19] M.K. De Armond, K.W. Hanck, D.W. Wertz, Coordn. Chem. 64 (1985) 65.

[20] S.M. Molnar, G. Vallas, J.S. Bridgewater, K.J. Brewer, J. Am. Chem. Soc. 116 (1994) 5206.
[21] P. Liska, N. Vlachopoulos, M.K. Nazeeruddin, P. Comte, M. Gratzel, J. Am. Chem. Soc. 110 (1988) 3686.
[22] K. Kalyanasundram, Photochemistry of Polypyridine and Porphyrin Complexes, Academic Press, London, 1992.
[23] A. Juris, V. Balzani, F. Barigellalti, S. Campagna, P. Belser, A. Von Zelewsky, Coordn. Chem. Rev. 84 (1988) 85.
[24] T.J. Meyer, Pure Appl. Chem. 58 (1986) 1193.
[25] J. DeSilvestro, M. Gratzel, L. Karan, J. Moser, J. Augustynski, J. Am. Chem. Soc. 107 (1985) 2988.
[26] N. Vlachopoulos, P. Liska, J. Augustynski, M. Gratzel, J. Am. Chem. Soc. 110 (1988) 1216.
[27] R. Amadelli, R. Argazzi, C.A. Bignozzi, F. Scandola, J. Am. Chem. Soc. 112 (1990) 7099.
[28] M.K. Nazeeruddin, P. Liska, J. Moser, N. Vlachopoulos, M. Gratzel, Helv. Chim. Acta 73 (1990) 1788.
[29] C.A. Bignozzi, R. Argazzi, M.T. Indelli, F. Scandola, Sol Energy Mater. Sol. Cells 32 (1994) 229.
[30] R. Argazzi, C.A. Bignozzi, T.A. Heimer, F.N. Castellano, G.J. Meyer, Inorg. Chem. 33 (1994) 5741.
[31] M.K. Nazeeruddin, P. Pechy, M. Gratzel, Chem. Commun. (1997) 1705.
[32] O. Kohle, S. Ruile, M. Gratzel, Inorg. Chem. 35 (1996) 4779.
[33] P. Hoyer, H. Weller, J. Phys. Chem. 99 (1995) 14096.
[34] K. Schwarzburg, F. Willig, Appl. Phys. Lett. 58 (1991) 2520.
[35] G. Schlichthorl, N.G. Park, A.J. Frank, J. Phys. Chem. B 103 (1999) 782.
[36] A. Solbrand, A. Henningsson, S. Sodergren, H. Lindstorm, A. Hagfeldt, S.E. Lindquist, J. Phys. Chem. B 103 (1999) 1078.
[37] A.C. Fisher, L.M. Peter, E.A. Ponomarev, A.B. Walker, K.G.U. Wijayantha, J. Phys. Chem. B 104 (2000) 949.
[38] N.W. Duffy, L.M. Peter, K.G.U. Wijayantha, Electrochem. Commun. 2 (2000) 262.
[39] P. Hemmerich, Bioinorganic Chemistry, Vol. II, American Chemical Society, Washington, DC, 1977, p. 312.
[40] P. Hemmerich, J. Lauterwein, Inorganic Biochemistry, Elsevier, New York, 1973, p. 1168.
[41] O. Groudinsky, Flavins and Flavoproteins, University Park Press, Baltimore, MD, 1970, p. 581.
[42] S.J. Benkovic, Annu. Rev. Biochem. 49 (1980) 227.
[43] R.L. Blakeley, The Biochemistry of Folic Acid and Related Pteridines, Elsevier, New York, 1969.
[44] P. Van Beelen, J.W. Van Neck, R.M. de Cock, G.D. Vogels, W. Guijt, C.A.G. Haasnoot, Biochemistry 23 (1984) 4448.
[45] D. Dolphin, Adv. Chem. Ser. 191 (1980) 65.
[46] W. Pfleiderer, Biochemical and Clinical Aspects of Pteridines, DeGruyter, Berlin, 1982.
[47] R.L. Blakely, L. Cocco, Biochemistry 24 (1985) 4702.
[48] W. Pfleiderer, E. Taylor, Pteridine Chemistry, Pergamon Press, Oxford, 1964.
[49] D.E. Wallick, L.M. Bloom, B.J. Grafney, S.J. Benkovic, Biochemistry 23 (1984) 1295.
[50] T.A. Dix, G.E. Bollag, P.L. Domanico, S.J. Benkovic, Biochemistry 24 (1985) 2955.
[51] S.O. Pember, J.J. Villafranca, S.J. Benkovic, Biochemistry 25 (1985) 6611.
[52] A. Albert, J. Biochem. 47 (1950) 9.
[53] D.J. Vonderschmitt, K.G. Scrimgeour, Biochem. Biophys. Res. Commun. 28 (1967) 302.
[54] K.B. Jacobson, J. Ferre, J.E. Caton, Bioorg. Chem. 13 (1985) 296.
[55] P. Hemmerich, Helv. Chim. Acta 47 (1964) 464.
[56] M.J. Clarke, M.G. Dowling, A.R. Garafalo, T.F. Brennan, J. Am. Chem. Soc. 101 (1979) 223.
[57] T.D. Wade, C.J. Fritchie, J. Biol. Chem. 248 (1973) 2337.
[58] J. Selbin, J. Sherrill, C.H. Bigger, Inorg. Chem. 14 (1974) 1736.
[59] B.J. Gallagher, T.L. Riechel, Inorg. Chim. Acta 66 (1982) 73.
[60] D.T. Sawyer, J.N. Gerber, L.W. Amos, L.J. DeHayes, J. Less-Common Met. 36 (1974) 487.
[61] M.W. Yu, C.J. Fritchie, J. Biol. Chem. 250 (1975) 946.
[62] C.J. Fritchie, J. Biol. Chem. 248 (1973) 7516.
[63] S.J.N. Burgmayer, A. Baruch, S. Brodie, A. Jafri, J. Perkinson, K. Yoon, in: Proceedings of the 195th National Meeting of the American Chemical Society, Toronto, Canada, 1988.
[64] S.J.N. Burgmayer, E.I. Stiefel, J. Am. Chem. Soc. 108 (1986) 8310.
[65] M.J. Clarke, M.G. Dowling, A.R. Garafalo, T.F. Brennan, J. Biol. Chem. 255 (1980) 3472.
[66] G. Subramanian, J.G. Mc Afee, J. Nucl. Med. 11 (1970) 365.
[67] M. Tanabe, Radioisotopes 25 (1976) 44.
[68] M. Wenzel, E. Nipper, W. Close, J. Nucl. Med. 18 (1977) 367.
[69] T.J. Meyer, Pure Appl. Chem. 58 (1986) 1193.
[70] R. Argazzi, C.A. Bignozzi, T.A. Heimer, F.N. Castellano, G.J. Meyer, J. Phys. Chem. B 101 (1997) 2591.
[71] D.D. Perrin, W.L. Armarego, D.R. Perrin, Purification of Laboratory Chemicals, 2nd Edition, Pergamon Press, Oxford, 1980.
[72] N. Garelli, P. Vierling, J. Org. Chem. 57 (1992) 3046.
[73] N. Vlachopoulos, P. Liska, J. Augustynski, M. Gratzel, J. Am. Chem. Soc. 110 (1988) 1216.
[74] M.K. Nazeeruddin, E. Muller, R. Humphry-Baker, N. Vlachopoulos, M. Gratzel, J. Chem. Soc., Dalton Trans. (1997) 4571.
[75] H. Taube, Surv. Prog. Chem. 6 (1973) 1.
[76] H.S. Lin, J. Barclay, F.C. Anson, Inorg. Chem. 11 (1972) 1460.
[77] E.L. Yee, R.J. Cave, L.G. Kendall, P.D. Tyma, M.J. Weaver, J. Am. Chem. Soc. 101 (1979) 1131.
[78] A.M. Zwickel, C. Creutz, Inorg. Chem. 10 (1971) 2395.
[79] J.A. Baiano, D.L. Carlson, G.M. Wolosh, D.E. DeJesus, C.F. Knowles, E.G. Szabo, W.R. Murphy Jr., Inorg. Chem. 29 (1990) 2327.
[80] M. Goodgame, M.A. Schmidt, Inorg. Chim. Acta 36 (1979) 151.
[81] K. Nakomoto, Infrared Spectra of Inorganic and Coordination Compounds, Wiley, New York, 1963.
[82] A.R. Katritzky, Physical Methods in Heterocyclic Chemistry, Vol. II, Academic Press, New York, 1963.
[83] J. Cunningham, G. Al Sayyed, J. Chem. Soc., Faraday Trans. 86 (1990) 3935.
[84] H.P. Boehm, Discuss. Faraday Soc. 52 (1971) 264.
[85] D. Duonghong, N. Serpone, M. Gratzel, Helv. Chim. Acta 67 (1984) 1012.
[86] D.A. Gulino, H.G. Drickamer, J. Phys. Chem. 88 (1984) 1171.
[87] D.N. Furlong, D. Wells, W.H.F. Sasse, J. Phys. Chem. 90 (1986) 1107.
[88] K. Kalyanasundaram, M.K. Nazeeruddin, Chem. Phy. Lett. 4 (1992) 193.
[89] R.H. Hage, J.G. Haasnoot, J. Reedijk, R. Wang, J.G. Vos, Inorg. Chem. 30 (1991) 3263.
[90] M.J. Powers, R.W. Callahan, D.J. Salmon, T.J. Meyer, Inorg. Chem. 15 (1976) 4.
[91] A.C. Lees, B. Evrard, T.E. Keyes, J.G. Vos, C.J. Kleverlaan, M. Alebbi, C.A. Bignozzi, Eur. J. Inorg. Chem. (1999) 2309.
[92] H. Yanagi, Y. Kanbayashi, D. Schlettwein, D. Wohrle, N.R. Armstrong, J. Phys. Chem. 98 (1994) 4760.
[93] R.C. Weast, M.J. Astle (Eds.), Handbook of Chemistry and Physics, CRC Press, Boca Raton, FL, 1979, p. E-85.